uc3m | Universidad Carlos III de Madrid

e-Archivo

This is a postprint version of the following published document:

Izquierdo Barrientos, M.A., Fernández Torrijos, M., Almendros Ibáñez, J.A. y Sobrino. C. (2016). Experimental study of fixed and fluidized beds of PCM with an internal heat exchanger. *Applied Thermal Engineering*, 106, pp. 1042-1051.

DOI: 10.1016/j.applthermaleng.2016.06.049

Research Paper

Experimental study of fixed and fluidized beds of PCM with an internal heat exchanger

M.A. Izquierdo-Barrientos [a], M. Fernández-Torrijos [a], J.A. Almendros-Ibáñez [b,c], C. Sobrino [a,*]

[a] Universidad Carlos III de Madrid, Departamento de Ingeniería Térmica y de Fluidos, Avda. de la Universidad 30, 28911 Leganés, Madrid, Spain
[b] Escuela de Ingenieros Industriales, Dpto. de Mecánica Aplicada e Ingeniería de Proyectos, Castilla-La Mancha University, Campus universitario s/n, 02071 Albacete, Spain
[c] Renewable Energy Research Institute, Section of Solar and Energy Efficiency, C/ de la Investigación s/n, 02071 Albacete, Spain

A R T I C L E   I N F O

H I G H L I G H T S

- Measured heat transfer coefficient between a bed of PCM and an immersed coil.
- Three different helical coil heat exchangers tested.
- Higher heat transfer coefficient for the fluidized bed than for the fixed bed.
- Higher heat transfer coefficient for the PCM than for a sensible heat material.

G R A P H I C A L   A B S T R A C T
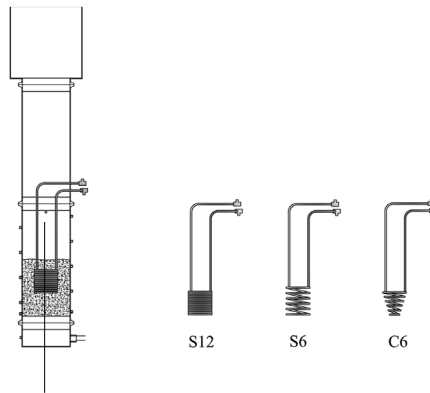
Keywords:
Fixed bed
Fluidized bed
Phase change material
Energy storage
Coil
Heat exchanger

A B S T R A C T

This work presents the results of experiments performed in a thermal energy storage tank filled with particles, which was heated using hot air and then discharged with a cold water stream circulating inside a heat exchanger immersed in the bed. Both fixed- and fluidized-bed configurations were studied. The materials used were sand, which is a material commonly employed in sensible heat storage, and a granular phase change material (PCM), in which the phase change occurs over the temperature range of 40–50 °C. Three different heat exchangers with different helical coil geometries were tested by measuring the temperatures in the bed and at the water inlet and outlet. Higher heat transfer coefficients between the bed and the water flow and higher heat exchanger effectiveness were observed for the heat exchanger with the greatest distance between coils, as it allows better contact between the bed particles and the heat exchanger surface when the particles are fluidized.

1. Introduction

Waste heat recovery and solar thermal energy systems are the primary applications for thermal energy storage (TES). Rock or sand beds have approximately half the volumetric heat capacity of water, and they require approximately 3.5 times as much space as an equivalent amount of heat in water due to the air space between the solid particles. However, rock TES systems are generally preferred in air-based systems and present some advantages over water because they can be used for TES over 100 °C, the problems associated with the water freezing in the collectors are avoided, their cost is lower than the cost of water containment in tanks, and the maintenance and capital costs of air collectors are lower compared with those of liquid collectors [1]. Space heating and ventilation air heating are two of the most common

applications of solar air systems [2]. In packed-bed solar energy storage systems, a heated fluid (typically air) flows from solar collectors into a bed of particles, in which thermal energy is transferred during the charging phase [3]. Most conventional packed bed storage systems separate the charging and discharging process, although operation strategies that allow simultaneous room heating and charging of the storage tank have also been proposed [2]. Packed beds generally employ rocks or sand as the storage material, storing the thermal energy in the form of sensible heat. However, granular phase-changing composites with small particle diameters (1–3 mm) have previously been tested in latent heat storage packed beds [4,5]. These materials consist of a natural porous matrix bound with an organic PCM. In this manner, the thermal energy is stored in the form of latent heat when the material changes from solid to liquid. The inorganic matrix that contains the PCM retains it when it is in the liquid phase, and thus, working with a liquid itself is avoided. The advantages of using a PCM are that the heat capacity increases and the temperature of the storage system can be maintained in a narrow range. Belmonte et al. [6] integrated a fixed-bed PCM tank into the heat rejection loop of absorption chillers, eliminating the wet cooling tower in the system and using a dry cooling tower combined with the PCM tank. Álvarez et al. [7] also used PCM properly located in the core of a mechanically ventilated air layer to improve the natural cooling in buildings and reduce the shift between the time when cool is stored and time when it is demanded by the building.

Similar to packed beds, fluidized beds can also be utilized integrated in different energy systems of buildings. For example, Chen et al. [8,9] used a fluidized bed system of silica gel for air conditioning in buildings. They observed an improve of 20% in the adsorption/desorption compared to a packed bed system. Zhou et al. [10] integrated a fluidized bed heat exchanger in a system for the production of CO_2 hydrate slurry in a cold storage system. The authors observed an improve between 23% and 43% of the COP of the system compared with a conventional system. Liquid/-solid fluidized bed heat exchangers have been also tested to exchange heat between a geothermal fluid and water in geothermal distric heating systems, and the thermal perfomance enhanced compared to the classic plate type heat exchanger [11]. The same granular PCM mentioned above was used by Izquierdo-Barrientos

et al. [5] in a fluidized-bed storage tank, and a higher charging efficiency was observed during the charging process for the fluidized bed compared to the same tank working under fixed-bed conditions. Moreover, the measured heat transfer coefficients to a horizontal cylindrical surface immersed in the bed were higher for the fluidized bed than for the fixed bed and for a granular PCM bed than for a bed of sand used as a reference material [12]. The tested granular PCM, which had a phase change temperature of approximately 50 °C, did not present agglomeration problems, and although it suffered some attrition after 75 h of continuous operation with 15 charging-discharging cycles, no evidence of PCM loss was observed, and the energy storage capacity of the fluidized particles was unaffected [13].

The idea of combining air with water heating systems has previously been developed in different solar energy applications. For example, Choudhury and Garg [14] studied a residential heating system in which solar water collectors were used to heat water to cover the domestic hot water demand of a four-person residential building. The hot water was stored in a cylindrical tank enclosed within an insulated rectangular tank, the annular space of which was filled with spherical rocks with a size of 0.03 m. In this manner, the tanks served as a water-to-air heat exchanger, in which a flow of air was circulated through the rock bed, absorbing heat from the water, and then it was used to heat the apartment. This system aims to provide a portion of the energy needs for domestic hot water without a significant reduction in the solar energy supply for space heating needs. Conventional air-rock solar systems for space heating see service only during the heating season. Adding domestic hot water capability to the basic air-rock system can provide 100% of the domestic hot water during summer and less during other seasons [1]. A different concept of an air-to-water solar hybrid heating system was studied by Choudhury and Garg [15], which consisted of an air solar collector, a finned-tube air–water heat exchanger and a water storage tank connected to the heat exchanger for storing hot water. A similar concept was presented by Misra [16], who evaluated a hybrid air and water heating system, in which air circulated in a closed loop with an air solar collector where the air was heated, and then it heated water in an air–water heat exchanger. The hot water was stored in a water storage tank and eventually an auxiliary heater was used
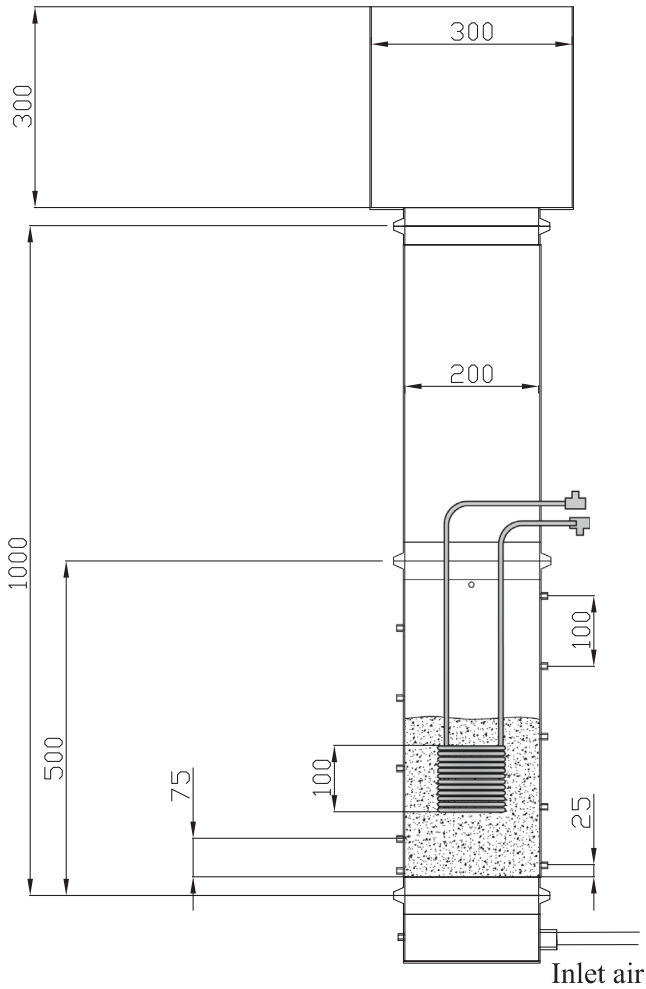
Fig. 1. Scheme of the experimental apparatus. Dimensions in mm.

Fig. 3. Specific heat variation as a function of temperature for sand and the granular PCM GR50.

to heat the water taken from the storage tank to a desired temperature. Regardless of the configuration, hybrid water–air heating systems require a heat exchanger, which is where the heat transfer between both fluids is accomplished. Heat transfer coefficients for gases are low; thus, fluidized-bed heat exchangers are a suitable option for increasing the heat transfer coefficient of the air side [17,18].

In this paper, a solid media storage tank with an internal heat exchanger is studied. The tank is charged using a hot air flow, and then the heat stored in the solid granular material is recovered by a water stream circulating inside the heat exchanger immersed in the bed of particles. The inlet and outlet temperatures of the air and water streams are measured to analyze the performance of the air–water heat exchanger. A granular PCM is employed as the solid

Fig. 2. Scheme of the different heat exchangers. Dimensions in mm.

(a) Sand S6   (b) PCM S6

(c) Sand S12   (d) PCM S12

(e) Sand C6   (f) PCM C6
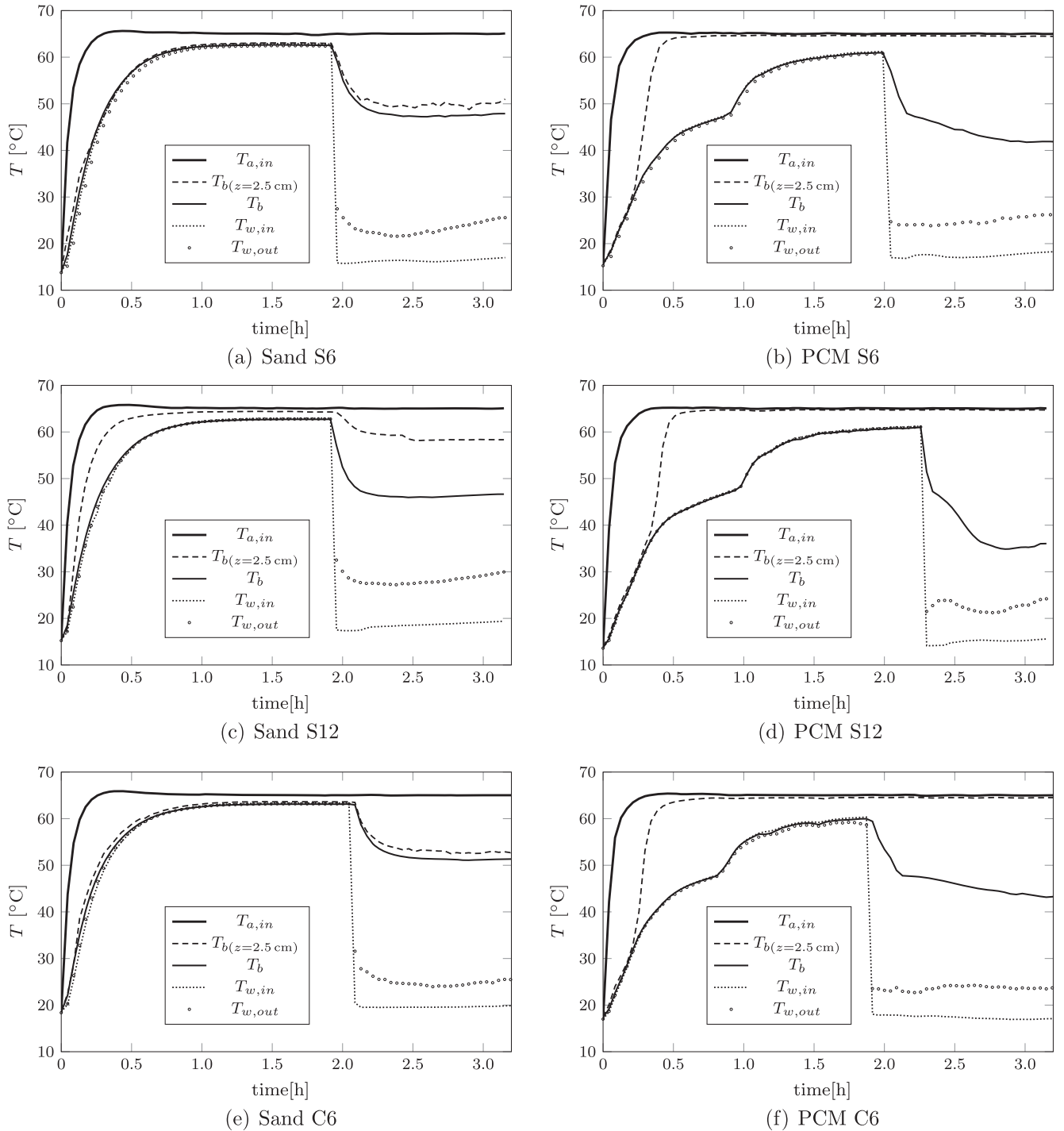
Fig. 4. Temperature profiles for the water and the fluidized beds of sand (Q = 750 l/min) and PCM (Q = 500 l/min).

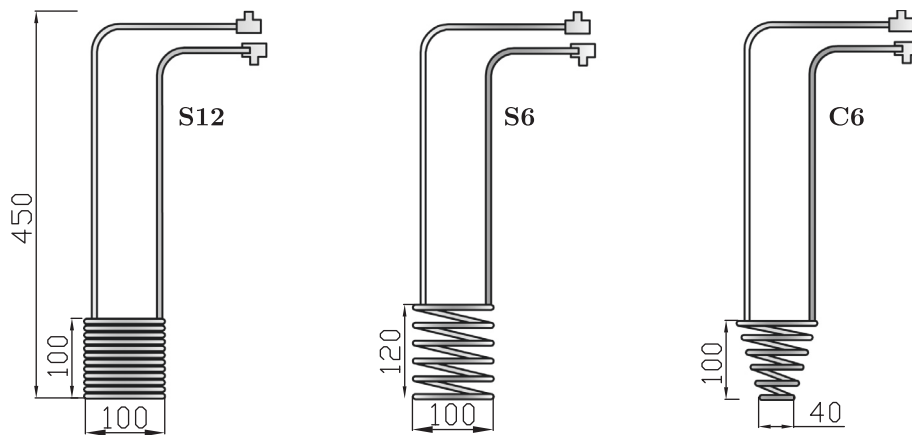material in the packed-bed storage tank, and its behavior is compared with sand, which is a material commonly employed in sensible heat packed-bed storage systems. Additional experiments were performed using the same materials but working under fluidized-bed conditions to enhance the heat transfer between the air flowing through the bed of particles and the water circulating inside the heat exchanger immersed in the bed. The system studied in this work would be able to exchange heat between an air and a water stream and additionally, store heat in the bed of solid material. Thus, the outlet air from the storage tank could be used for space heating, while the excedent heat not needed to

cover the heating load could be used to cover the domestic hot water demand, assisted by an auxiliary heater when needed.

2. Materials and experimental apparatus

Experiments were conducted using the experimental set-up shown in Fig. 1. The fluidized-bed column is a cylinder with an internal diameter of 0.2 m and a height of 0.5 m, and it is insulated with 2-cm-thick glass wool. An air stream produced by a blower is heated to a temperature of 65 °C by electrical heaters and enters the bed crossing a distributor plate with a 3% open area, which

4

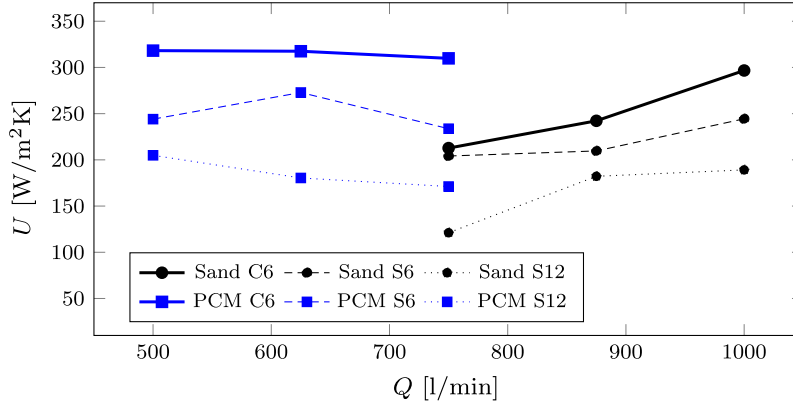**Fig. 5.** Overall heat transfer coefficient between the fluidized bed and the water.
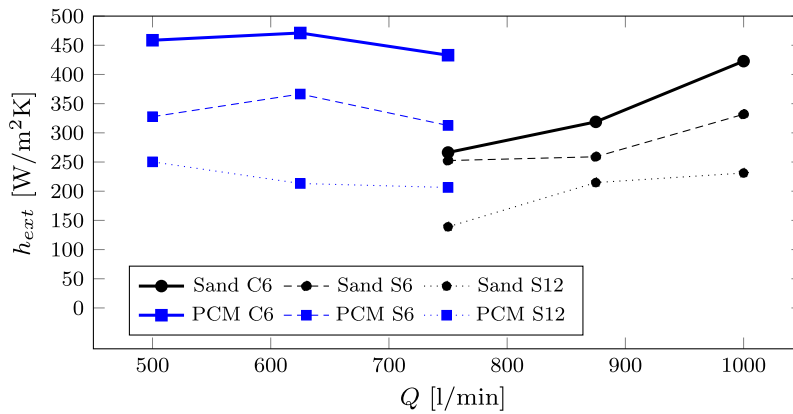

Fig. 6. Convection heat transfer coefficient between the fluidized bed and the heat exchanger surface.

ensures a uniform distribution of the gas in the bed. Several ports at different heights and radial positions are placed in the bed column wall to allow the installation of type K thermocouples. A stainless steel helical coil heat exchanger is submerged in the bed. Cold water flows inside the coils and it is heated by the hot bed. Fig. 2 shows the three different types of helical coil heat exchangers tested in this work: a heat exchanger with 12 coils of 10 cm diameter and 10 cm height (S12), a heat exchanger with 6 coils of 10 cm diameter and 12 cm height (S6) and a heat exchanger with 6 coils of decreasing diameter from 10 cm at the top to 4 cm at the bottom and 10 cm height (C6). The distance between coils in heat exchanger S6 is greater than that in heat exchanger S12, allowing better contact between the bed particles and the coil external surface. Heat exchanger C6 also allows better contact because each coil is not impeded by neighboring coils, although the heat transfer surface is reduced. Table 1 summarizes the main dimensions of the three heat exchangers.

Experiments were performed using the bed in fixed and fluidized conditions. Sand, which is a typical material employed in packed and fluidized beds, and a granular PCM were used as the bed material, and both of these materials are available in two different particle sizes. The granular PCM (GR50), commercialized by Rubitherm, changes its phase in the temperature range of 40–50 °C and is available in two sizes with particle diameters between 1–3 mm and 0.2–0.6 mm. The material that changes its phase is paraffin, and it is bound within a secondary supporting structure of SiO_2. For the sand and granular PCM, the finer grades were used in the fluidized-bed experiments, whereas the coarser grades were employed for the fixed-bed conditions. The finer grades were not used in the fixed-bed experiments because the air velocity that

should be applied to maintain the bed under fixed-bed conditions would be too low. Thus, the coarser grades permit the same materials to be used with higher gas velocities. In both the fluidized- and fixed-bed experiments, the bed was filled with 5 kg of PCM or with 9 kg of sand. In both cases, the height of the bed of particles was 0.24 m. Table 2 summarizes some properties of the solid materials, such as the density, mean particle diameter and its standard deviation and the bed voidage, and Fig. 3 shows the variation in the specific heat with temperature for each material.

3. Results and discussion

Experiments with the different heat exchanger geometries and materials in fixed- and fluidized-bed conditions were conducted to investigate the influence on the heat transfer between the bed and the heat exchanger surface.

3.1. Fluidized-bed experiments

To fluidize the bed, the superficial air velocity needs to be higher than the minimum fluidization velocity of the material, U_{mf}. This velocity was experimentally measured following the methodology proposed by Sánchez-Delgado et al. [19], and a value of $U_{mf} = 0.13$ m/s was obtained for the finer GR50, which corresponds to a flow rate of 250 l/min. For the finer sand, the velocity was $U_{mf} = 0.27$ m/s, which was obtained with a flow rate of 500 l/min. In each experiment, the bed was heated to a temperature of 65 °C using hot air. Once the bed reached this temperature, cold water at a constant flow rate of approximately 0.4 l/min was circu-
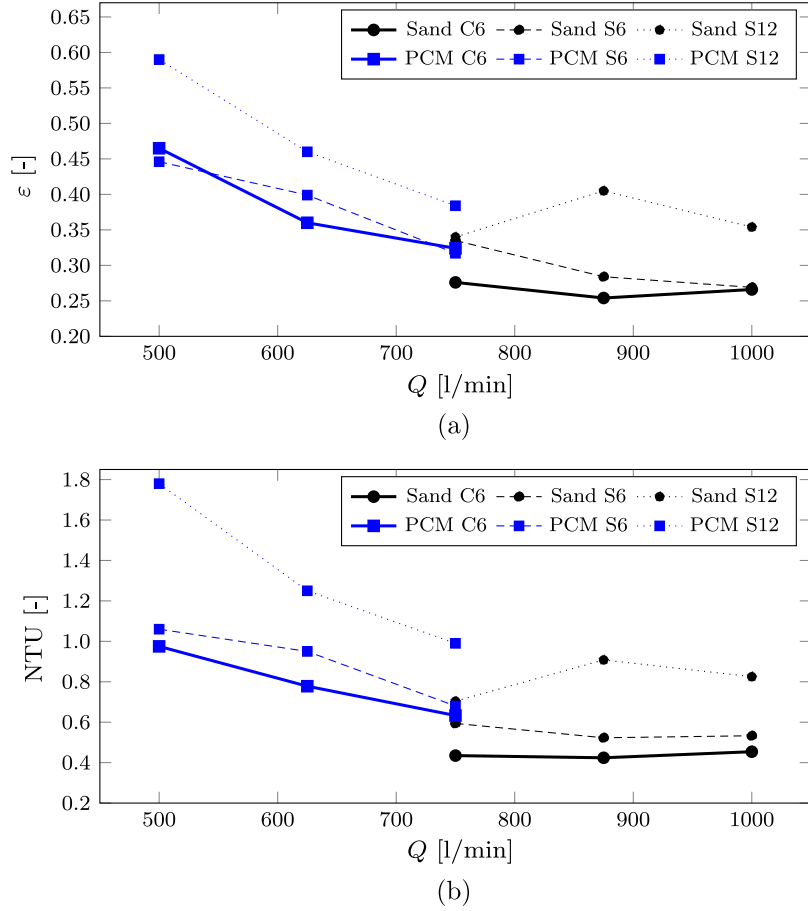
5

Fig. 7. Fluidized-bed heat exchanger (a) effectiveness and (b) *NTU*.

lated and heated inside the coil immersed in the bed. The temperature of the air at the bed inlet was maintained at 65 °C throughout the entire experiment. The experiments with sand were performed using different air flow rates. The time evolutions of the temperature inside the bed, T_b, the inlet water temperature, $T_{w,in}$, and the outlet water temperature, $T_{w,out}$, are shown in Fig. 4. The feeding air temperature measured in the plenum chamber, $T_{a,in}$, is also presented in this figure. The air flow rate for the sand was 750 l/min, which corresponds to a superficial gas velocity of U_s = 0.4 m/s, with the ratio U_s/U_{mf} = 1.5. The air flow rate for the PCM bed was 500 l/min, which corresponds to a U_s = 0.27 m/s, with the ratio U_s/U_{mf} = 2. The temperatures measured at different heights inside the bed were the same because fluidized beds are well mixed and present a uniform temperature [5,12]. However, the thermocouple placed at 2.5 cm above the distributor measured an average temperature between the feeding air temperature and the bed temperature due to the air jets that are formed above the distributor [20]. After approximately 2 h, the temperature of the bed decreased when the water flow began, and the water was heated inside the heat exchanger due to the heat transferred from the bed. The water was heated to a higher temperature for heat exchanger S12 due to its higher heat transfer area. For the PCM bed, a small water temperature increase was observed when the bed material changed it phase, starting at approximately 49 °C.

The global heat transfer coefficient between the bed and the water for the fluidized bed experiments was calculated to compare the performance of the different heat exchanger geometries. The instantaneous logarithmic mean temperature, *LMTD*, for the heat exchanger, considering a uniform temperature of the fluidized bed, T_b, is

$$LMTD = \frac{(T_b - T_{w,out}) - (T_b - T_{w,in})}{\ln\left(\frac{T_b - T_{w,out}}{T_b - T_{w,in}}\right)} \tag{1}$$

where $T_{w,in}$ is the inlet water temperature and $T_{w,out}$ is the outlet water temperature. Then, the overall heat transfer coefficient between the water flowing inside the coil and the fluidized bed U can be calculated from

$$UA = \frac{\dot{m}_w c_{p,w}(T_{w,out} - T_{w,in})}{LMTD} \tag{2}$$

where $\dot{m}_w$ is the mass flow rate of water, $c_{p,w}$ is its specific heat, and A is the heat transfer area.

The values of the overall heat transfer coefficient for the different coils as a function of the air flow rate are presented in Fig. 5. The cone-shaped heat exchanger, C6, presents the highest heat transfer coefficient. In addition, the heat exchanger with a greater distance between coils, S6, presents a higher heat transfer rate than heat exchanger S12 due to the better contact between the bed particles and the external surface of the heat exchanger, which is limited in the case of coil S12 because there is not space between coils to allow the particles to freely move. Moreover, higher heat transfer coefficients are observed for the PCM than for the sand, despite the lower air flow rate, because the latent heat stored by the PCM particles is released when they are cooled by the flowing water. The same behavior was reported by Izquierdo-Barrientos et al. [12] for experiments performed introducing a heat transfer sensor with resistance heating in a cold bed.

The convection heat transfer coefficient between the fluidized bed and the external surface of the coil was calculated from the overall heat transfer coefficient U, neglecting the conduction resis-
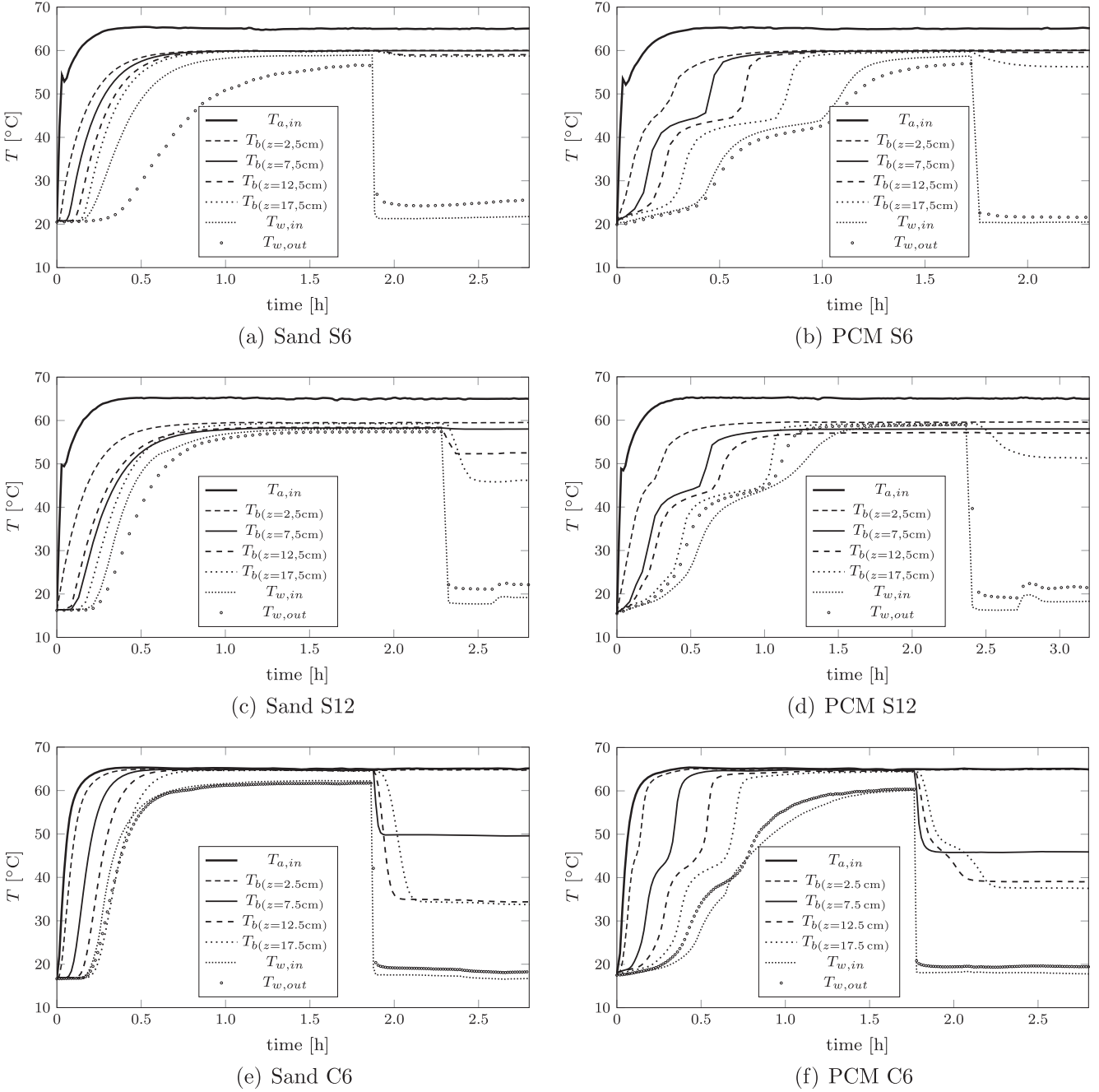
6

Fig. 8. Temperature profiles for the water and the fixed bed for a flow rate $Q = 500$ l/min.

tance of the pipe and estimating the internal flow convection coefficient using the correlation proposed by Manlapaz and Churchill [21] for laminar flow in helical coils subjected to constant temperature boundary conditions. This coefficient is shown as a function of the air flow rate in Fig. 6 for the different coils immersed in the fluidized bed of sand or PCM. The behavior of the external heat transfer coefficient is similar to that observed for the global heat transfer coefficient in Fig. 5.

Fig. 6 shows that the heat transfer coefficient for the granular PCM appears to reach the maximum value in the range of flow rates shown in this figure. In contrast, the heat transfer coefficient of the sand linearly increases to the maximum tested flow rate of 1000 l/min. The flow rate that obtains the maximum heat transfer

coefficient can be estimated according to Todes' correlation [22–24]:

$$Re_{\max} = \frac{Ar}{18 + 5.2\sqrt{Ar}} \tag{3}$$

where $Ar = \left(d_p^3 \rho_a (\rho_s - \rho_a) g\right)/\mu_a^2$ is the Archimedes number. For the materials used in this work, the Archimedes number is $Ar \gtrsim 10^3$, and for this high value, Eq. (3) indicates that $Re_{\max} \propto \sqrt{Ar}$. The density of the sand is higher than that of the PCM, although their particle sizes are similar, and consequently, $Ar_{\text{sand}} > Ar_{\text{PCM}}$ and $Re_{\max_{\text{sand}}} > Re_{\max_{\text{PCM}}}$. Izquierdo-Barrientos et al. [12] observed similar results using a cylindrical heat transfer probe,

7

obtaining $Re_{\max_{PCM}} \approx 600 - 700$ l/min, whereas the heat transfer coefficient for the sand increased linearly up to a flow rate of 1000 l/min.

The heat exchanger effectiveness ε has been defined as [17]

$$\varepsilon = \frac{\dot{m}_w c_{p,w}\left(T_{w,out} - T_{w,in}\right)}{\dot{m}_a c_{p,a}\left(T_{a,in} - T_{w,in}\right)} \tag{4}$$

where $\dot{m}_a$ is the mass flow rate of air in the bed and $c_{p,a}$ is its specific heat.

Fig. 7 presents the heat exchanger effectiveness and the parameter $NTU = UA/C_{min}$ for the different heat exchangers in a fluidized bed of sand or PCM, where C_{min} is the heat capacity of the fluid with a smaller heat capacity, which is the air for all the experiments presented in this work. The effectiveness for the coil submerged in a PCM bed is higher than for the sand. This result is consistent with the results reported by Suo [17], who observed that the effectiveness increases with NTU and decreases with the ratio C_{min}/C_{max}. The system with PCM has higher NTU values and a lower air mass flow rate than in the case of sand. Heat exchanger S12 presents the highest effectiveness among the three heat exchangers tested because it has a higher heat transfer area (see Table 1) and consequently, higher NTU values for the same air flow rate. The differences in effectiveness between heat exchangers S6 and C6 are smaller, particularly for the case with PCM, with similar values of effectiveness. Heat exchanger C6 has a higher heat transfer coefficient (see Fig. 6) because its geometry permits better contact with the particles. However, the heat transfer area of heat exchanger S6 is higher, resulting in similar values of NTU and consequently, similar values of the effectiveness for the same air flow rate.

3.2. Fixed-bed experiments

Additional experiments were conducted using the different heat exchangers immersed in the bed of particles (sand or PCM) and operated below U_{mf} to have a fixed-bed configuration. Fig. 8 presents the temperature measured at different heights in the bed during the charging of the bed to a temperature of 65 °C for the sand or PCM with the different types of heat exchangers, with an air flow rate of 500 l/min. The inlet temperature of the bed is also presented in this figure. After approximately two hours of continuous operation, where all the temperatures measured in the bed are at steady state, the water starts to flow within the coils, and the inlet and outlet water temperatures are also measured. In this case, the temperature decreases linearly along the bed height. This stratification is an advantage if the storage tank is going to be integrated with a solar heater because solar collectors operate at a higher effectiveness as the collector inlet temperature decreases

[1]. However, the temperature increase of the water in this case is lower because fixed beds present lower heat transfer coefficients to immersed surfaces than fluidized beds because in the latter, there is a continuous renovation of the particles in contact with the exchanger surface due to the action of the rising bubbles. Among the heat exchangers tested in these experiments, only heat exchanger C6 presented a high enough heat transfer rate to cool the bed of particles. Moreover, it can be concluded from the temperature measured at a height of 7.5 cm in the PCM bed (Fig. 8 (f)) that the lower part of the bed does not change its phase during discharging. This was not observed in the fluidized bed due to the temperature uniformity achieved by the mixing effect of the rising bubbles.

The instantaneous logarithmic mean temperature $LMTD$ for the coil, which is a counterflow heat exchanger, is defined as

$$LMTD = \frac{\left(T_{a,in} - T_{w,out}\right) - \left(T_{a,out} - T_{w,in}\right)}{\ln\left(\frac{T_{a,in} - T_{w,out}}{T_{a,out} - T_{w,in}}\right)}, \tag{5}$$

and then, the overall heat transfer coefficient between the water flowing inside the coil and the packed bed can be calculated using Eq. (2).

Fig. 9 presents this heat transfer coefficient U for the sand bed and the PCM bed for the different heat exchangers as a function of the air flow rate. The benefit expected in the heat transfer coefficient resulting from the phase change of the PCM is limited because there is no movement of the particles surrounding the coil surface, and only the latent heat released by those particles surrounding the coil is transferred to the water. Although the heat transfer rate is not sufficient to cool the bed below the phase change temperature in some experiments, not even for the coil C6, where the bed temperature decreases below this transition temperature (Fig. 8(f)), an increase in the heat transfer coefficient due to the PCM is observed. In contrast, higher heat transfer coefficients are observed for the sand because it has a lower particle size than the coarse GR50. In accordance with this result, Izquierdo-Barrientos et al. [12] did not observe an increase in the heat transfer coefficient measured using a cylindrical heat transfer probe immersed in the bed of PCM compared with the sand under fixed-bed conditions. As previously observed for the fluidized bed, the heat transfer coefficient increases with the air flow rate. Comparing the values of the heat transfer coefficient for the different heat exchanger geometries, heat exchanger C6 has the highest coefficients and heat exchanger S12 presents the lowest, as also observed for the fluidized bed (Fig. 5). Comparing the values of U for heat exchanger C6, the values for the fluidized bed of sand are twofold greater than those measured in the fixed bed of sand
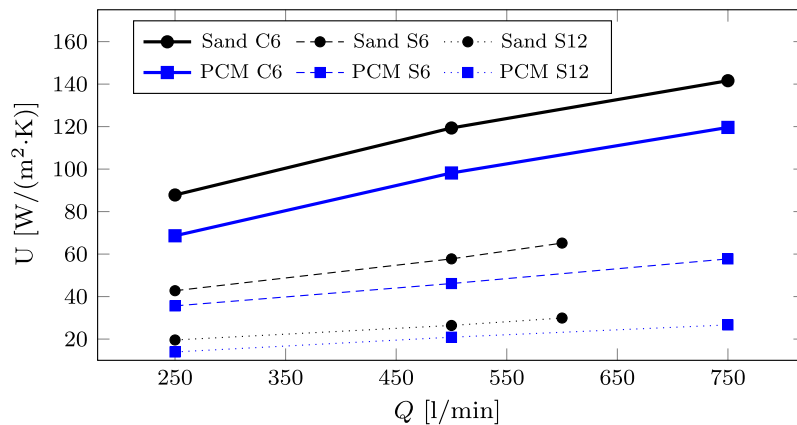

Fig. 9. Overall heat transfer coefficient between the fixed bed and the water.

or PCM, and the values for the fluidized bed of PCM are three times greater than the values of the fixed bed of sand or PCM.

Fig. 10 presents the values of the convection heat transfer coefficient between the external surface of the heat exchanger and the fixed bed of sand or PCM. This coefficient was calculated from the global heat transfer coefficients, as explained previously for the fluidized bed. The variation in this coefficient with the air flow rate and for the different coil geometries is similar to that observed for the global heat transfer coefficient in Fig. 9.

Fig. 11(a) shows the effectiveness of the different heat exchangers immersed in the fixed bed of sand or PCM as a function of the air flow rate, and Fig. 11(b) presents the corresponding NTU parameters. The effectiveness is lower than in the fluidized bed (Fig. 7(a)). In addition, it can be observed that the effectiveness decreases with the air flow rate because, although the heat transfer coefficient from the fixed bed to the coil surface increases, the heat capacity ratio C_{min}/C_{max} also increases, which consequently decreases the effectiveness. Comparing both materials, the
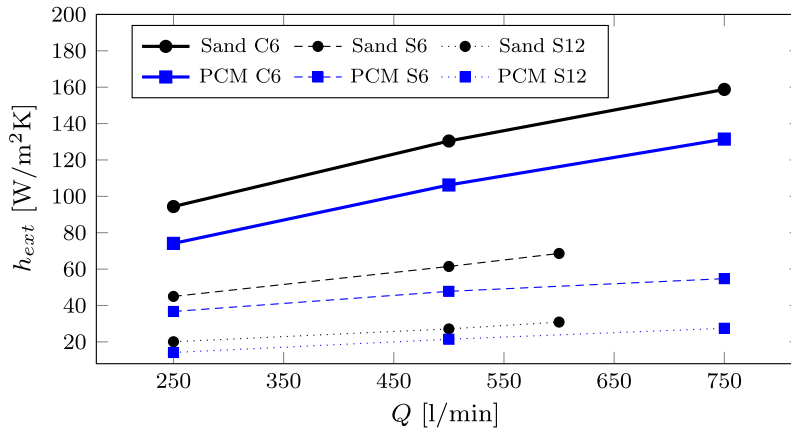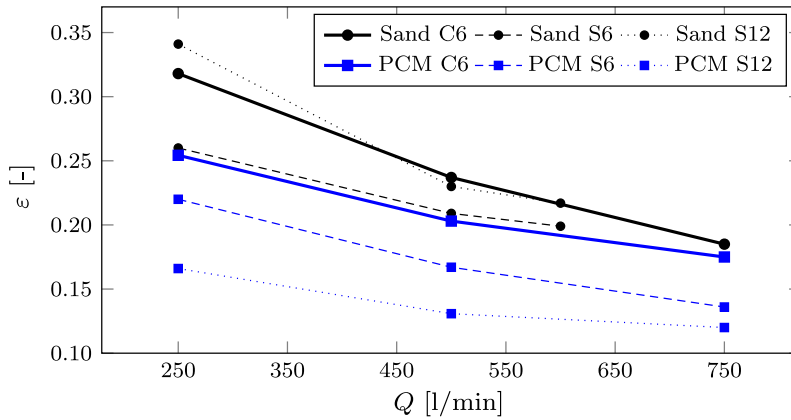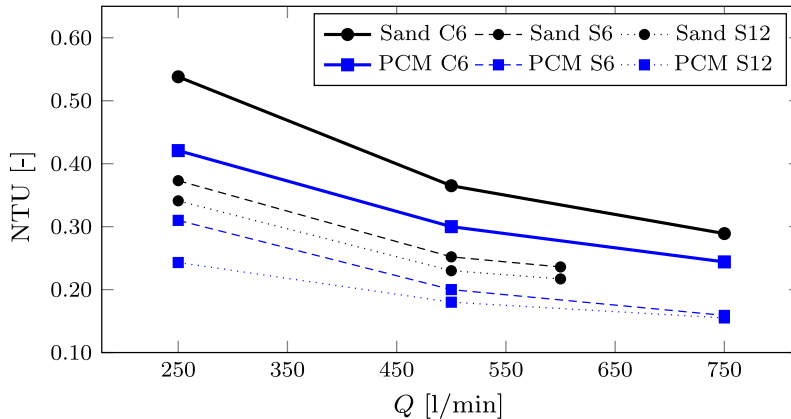

Fig. 10. Convection heat transfer coefficient between the fixed bed and the heat exchanger surface.

(a)

(b)

Fig. 11. Fixed-bed heat exchanger (a) effectiveness and (b) NTU.

effectiveness is higher for the sand due to the higher heat transfer coefficient caused by the smaller particle size. Heat exchangers C6 and S12 present similar effectivenesses, which are higher than the effectiveness of coil S6. This result occurs because the lower heat transfer area of coil C6 is counterbalanced by its higher external convection heat transfer coefficient, caused by the better contact between the particles and the coil surface.

4. Conclusions

Experiments were conducted using three different helical coil heat exchangers to recover the energy from a bed of solid particles heated with a flow of hot air. The bed was operated under fixed- and fluidized-bed conditions, and two different materials were tested: a granular PCM and sand, a material that is commonly employed in sensible heat storage tanks. Higher heat transfer coefficients and heat exchanger effectivenesses were measured for the heat exchanger geometry that allows better contact between the bed and the coil surface for the fluidized bed compared with the fixed bed and for the PCM compared with the sand. The increase in the heat transfer coefficient at the heat exchanger surface obtained with the PCM was not observed if the bed was under fixed-bed conditions. During the charging of the bed using hot air, the temperature was uniform for the fluidized bed, whereas it decreased linearly along the bed height for the fixed bed. To take advantage of the features of both fixed and fluidized beds, if the tank is going to be heated using hot air from solar air collectors, the charging of the bed should be performed while maintaining it in fixed-bed conditions to keep the bed stratification, while the heat recovery using water flowing inside an internal heat exchanger should be performed under fluidized-bed conditions to achieve higher heat transfer rates.

Acknowledgments

References

[1] I. Dincer, A.M. Rosen, Thermal Energy Storage: Systems and Applications, John Wiley & Sons, Chichester, 2002.
[2] D.L. Zhao, Y. Li, Y.J. Dai, R.Z. Wang, Optimal study of a solar air heating system with pebble bed energy storage, Energy Convers. Manage. 52 (2011) 2392–2400.
[3] H. Singh, R.P. Saini, J.S. Saini, A review on packed bed solar energy systems, Renew. Sust. Energy Rev. 14 (2010) 1059–1069.
[4] M. Rady, Granular phase change materials for thermal energy storage: experiments and numerical simulations, Appl. Therm. Eng. 29 (2009) 3149–3159.
[5] M.A. Izquierdo-Barrientos, C. Sobrino, J.A. Almendros-Ibáñez, Thermal energy storage in a fluidized bed of PCM, Chem. Eng. J. 230 (2013) 573–583.
[6] J.F. Belmonte, M.A. Izquierdo-Barrientos, P. Eguía, A. Molina, J.A. Almendros-Ibáñez, PCM in the heat rejection loops of absorption chillers: a feasibility study for the residential sector in Spain, Energy Build. 80 (2014) 331–351.
[7] S. Álvarez, L.F. Cabeza, A. Ruiz-Pardo, A. Castell, J.A. Tenorio, Building integration of PCM for natural cooling of buildings, Appl. Energy 109 (2013) 514–522.
[8] C.H. Chen, S.S. Ma, P.H. Wu, Y.C. Chiang, S.L. Chen, Adsorption and desorption of silica gel circulating fluidized beds for air conditioning systems, Appl. Energy 155 (2015) 708–718.
[9] C.H. Chen, G. Schmid, C.T. Chan, Y.C. Chiang, S.L. Chen, Application of silica gel fluidised bed for air-conditioning systems, Appl. Therm. Eng. 89 (2015) 229–238.
[10] H. Zhou, I. de Sera, C.I. Ferreira, Modelling and experimental validation of a fluidized bed based CO_2 hydrate cold storage system, Appl. Energy 158 (2015) 433–445.
[11] M.A.M. Tan, R. Karabacak, Experimental assessment the liquid/solid fluidized bed heat exchanger of thermal performance: an application, Geothermics 62 (2016) 70–78.
[12] M.A. Izquierdo-Barrientos, C. Sobrino, J.A. Almendros-Ibáñez, Experimental heat transfer coefficients between a surface and fixed and fluidized beds with PCM, Appl. Therm. Eng. 78 (2015) 373–379.
[13] M.A. Izquierdo-Barrientos, C. Sobrino, J.A. Almendros-Ibáñez, C. Barreneche, N. Ellis, L.F. Cabeza, Characterization of granular pcms for thermal energy storage applications in fluidized beds, Appl. Energy (2016). submitted for publication.
[14] C. Choudhury, H.P. Garg, Integrated rock bed heat exchanger-cum-storage unit for residential-cum-water heating, Energy Convers. Manage. 36 (1995) 999–1006.
[15] C. Choudhury, H.P. Garg, Performance calculations for closed-loop air-to-water solar hybrid heating systems with and without a rock bed in the solar air heater, Renew. Energy 3 (1993) 897–905.
[16] R. Misra, Evaluation of economic and thermal performance of closed loop solar hybrid air and water heating systems for indian climates, Energy Convers. Manage. 34 (1993) 363–372.
[17] M. Suo, Calculations methods for performance of heat exchangers enhanced with fluidized beds, Lett. Heat Mass Trans. 3 (1976) 555–564.
[18] O.M.H. Rodríguez, A.A.B. Pécora, W.A. Bizzo, Heat recovery from hot solid particles in a shallow fluidized bed, Appl. Therm. Eng. 22 (2002) 145–160.
[19] S. Sánchez-Delgado, J. Almendros-Ibáñez, N. García-Hernando, D. Santana, On the minimum fluidization velocity in 2D fluidized beds, Powder Technol. 207 (2011) 145–153.
[20] A.C. Rees, J.F. Davidson, J.S. Dennis, P.S. Fennell, L.F. Gladden, A.N. Hayhurst, M. D. Mantle, C.R. Müller, A.J. Sederman, The nature of the flow just above the perforated plate distributor of a gas-fluidised bed, as imaged using magnetic resonance, Chem. Eng. J. 61 (2006) 6002–6015.
[21] R.L. Manlapaz, S.W. Churchill, Fully developed laminar convection from a helical coil, Chem. Eng. Commun. 9 (1981) 185–200.
[22] M. Tsukada, M. Horio, Maximum heat transfer coefficient for an immersed body in a bubbling fluidized bed, Ind. Eng. Chem. Res. 31 (1992) 1147–1156.
[23] D. Sathiyamoorthy, M.R. Rao, Prediction of maximum heat transfer coefficient in gas fluidized bed, Int. J. Heat Mass Tran. 35 (1992) 1027–1034.
[24] J.R. Grace, B. Leckner, J. Zhu, Y. Cheng, Fluidized beds, in: C.T. Crowe (Ed.), Multiphase Flow Handbook, Taylor & Francis, Philadelphia, 2006. pp. 5-1–5-93.